

## Critical fan in the antiferromagnetic three-state Potts model

M. P. M. den Nijs, M. P. Nightingale, and M. Schick

*Department of Physics, FM-15, University of Washington, Seattle, Washington 98195*

(Received 2 March 1982)

The three-state Potts model on a square lattice with general nearest-neighbor interaction and ferromagnetic second-neighbor interaction is studied. At zero temperature the model with antiferromagnetic nearest-neighbor interactions is mapped to the  $F$  model. By comparing the excitations generated at nonzero temperature to those that lead to the eight-vertex model we obtain an explicit expression for the critical index describing such excitations and demonstrate the existence of a critical fan for ferromagnetic second-neighbor interactions. The model with purely nearest-neighbor interactions is critical only at zero temperature. Explicit expressions for the scaling indices of the color-color correlation function in the critical phase are also obtained. Phenomenological renormalization-group methods are applied to determine the general boundaries of the critical fan and to verify our expressions for critical indices. A physical system which might be expected to undergo a transition in the same universality class as that of the above model and to exhibit a critical phase is proposed: an equal mixture of krypton and xenon adsorbed on graphite.

### I. INTRODUCTION

There has been considerable interest recently in the antiferromagnetic three-state Potts model on a square lattice due to the possibility that it might exhibit a rather interesting phase transition. The idea that the nearest-neighbor model would undergo any transition is somewhat surprising in view of the lack of an obvious ground state. In fact it is known that the zero-temperature entropy of the system is extensive and is simply related to the entropy of the exactly soluble "square-ice" problem.<sup>1</sup> Nevertheless, it was suggested by Berker and Kadanoff<sup>2</sup> that models such as this could exhibit an entropy-driven transition to a critical phase characterized by a power-law decay of correlations. Such behavior in the antiferromagnetic three-state Potts model at zero temperature could already be inferred from the fact that the square-ice model<sup>1</sup> is critical, as it is a particular point of the six-vertex model<sup>3,4</sup> within its critical region. However, the above suggestion would imply this behavior at *nonzero* temperature as well. Cardy<sup>5</sup> showed that any transition of the antiferromagnetic Potts model would be in the universality class of the six-state clock model. This model is believed to exhibit two different behaviors depending on the parameters of the model: It undergoes either a simple first-order transition to an ordered phase or a sequence of two infinite-order Kosterlitz-Thouless transitions,<sup>6</sup> the first to a critical phase, the second to an ordered phase. Cardy claimed that the Potts model exhibits a transition of

the latter type at finite temperatures. Monte Carlo simulations<sup>7</sup> of this Potts model were carried out but were inconclusive. Recent phenomenological<sup>8</sup> and Monte Carlo<sup>9</sup> renormalization-group calculations strongly indicate that the system exhibits a transition only at zero temperature.

The introduction of a second-neighbor ferromagnetic interaction breaks the infinite ground-state degeneracy and brings about a transition to a phase with six equivalent ordered states, each characterized by two sublattices which are occupied by different Potts "colors." The two-component order parameter characterizing these states can be written

$$M_1 + iM_2 = \sum_j e^{i\theta_j} - \sum_k e^{i\theta_k},$$

where  $j$  is a site index on one sublattice,  $k$  an index on the other, and the variables  $\theta$  located on the sites can take the three "colors"  $0, \pm 2\pi/3$ . We consider in this paper such a three-state Potts model with arbitrary first-neighbor interaction  $K = \ln u$  and second-neighbor interaction  $L = \ln v$ . In general we take  $L$  ferromagnetic. We show that this model does indeed exhibit a critical phase for antiferromagnetic first-neighbor interactions. This is done in Sec. II by noting that in the limit  $u = 0$ , the system is isomorphic to the exactly soluble  $F$  model<sup>3</sup> with the parameter  $\Delta = 1 - v^2/2$ . From the fact that the  $F$  model is critical for all  $|\Delta| < 1$  and exhibits an infinite-order transition at  $\Delta = -1$  to a phase with long-range order we infer that, for  $u = 0$ , the Potts model is critical for all  $v < v_2 = 2$  and un-

dergoes a Kosterlitz-Thouless transition at  $v_2$  to the ordered phase. Next the effect of a finite but strong antiferromagnetic interaction ( $u \ll 1$ ) is investigated by examining the vortex excitations which arise when the constraint  $u = 0$  is relaxed. We find that these excitations introduced into the Potts model near the  $F$ -model limit are characterized by a vorticity which is  $\frac{3}{2}$  that of the excitations introduced into the eight-vertex model near its  $F$ -model limit. Because of the universality connection between the six-vertex and the Gaussian models,<sup>10-17</sup> the critical indices of different vortex operators obey extended scaling relations; in particular,

$$(2 - y_K) = \left(\frac{3}{2}\right)^2 (2 - y_{8v}), \quad (1.1)$$

where the singular part of the free energy behaves as

$$f(u, v) \sim u^{2/y_K}, \quad 0 < v < v_1. \quad (1.2)$$

From Baxter's solution of the eight-vertex model<sup>18</sup> we obtain

$$y_K = \frac{9}{2\pi} \mu(v) - \frac{5}{2}, \quad (1.3)$$

with

$$\mu = \cos^{-1} \left[ \frac{v^2}{2} - 1 \right], \quad 0 < \mu < \pi.$$

The vortex excitations in the Potts model are irrelevant for

$$v > v_1 = (2 + 2 \cos 5\pi/9)^{1/2} \simeq 1.29,$$

so that for small fixed values of  $u$  the Potts model exhibits an infinite-order transition into a critical phase at  $v = v_1$ . The second transition from this phase to the ordered phase at  $v = v_2$  is unaffected by these irrelevant excitations. Thus the presence of a critical phase for small  $u$  is established. We also

obtain the scaling indices in the critical phase of the color-color correlation function

$$\langle \cos(\theta_0 - \theta_i) \rangle \simeq \frac{A}{r^{2x_D}} \pm \frac{B}{r^{2x_S}}. \quad (1.4)$$

Here  $r$  is the distance between sites  $i$  and  $0$ , and the sign of the second term depends upon whether the two sites are on the same sublattice. We find

$$x_D = 4x_S, \quad (1.5)$$

$$x_S(2 - y_K) = \frac{1}{4}. \quad (1.6)$$

The phase boundaries for nonzero  $u$  are obtained in Sec. III by the application of a phenomenological renormalization-group procedure.<sup>19</sup> In particular the finite-size scaling behavior of the interfacial free energy is used to determine the temperatures at which the system is critical. The resulting boundaries of the ferromagnetic and antiferromagnetic phases are shown in Fig. 1. As shown there, the special case of the model with nearest-neighbor interactions is critical solely at  $T = 0$ . This follows from Eq. (1.3) with  $v = 1$  from which the vortex excitations are relevant. Near zero temperature the singular part of the free energy behaves as  $f(u, 1) \sim u^4 = \exp(4K)$ . In addition to the phase boundaries the critical exponent  $y_K$  is calculated and Eq. (1.3) is verified. The scaling indices  $x_D$  and  $x_S$  are also calculated on the boundaries of the critical fan, and the results are in good agreement with (1.5) and (1.6).

We conclude in Sec. IV with a brief discussion of a physical system which might be expected to undergo a transition in the same universality class as that of the antiferromagnetic Potts model and to exhibit a critical phase: an equal mixture of krypton and xenon adsorbed on graphite.

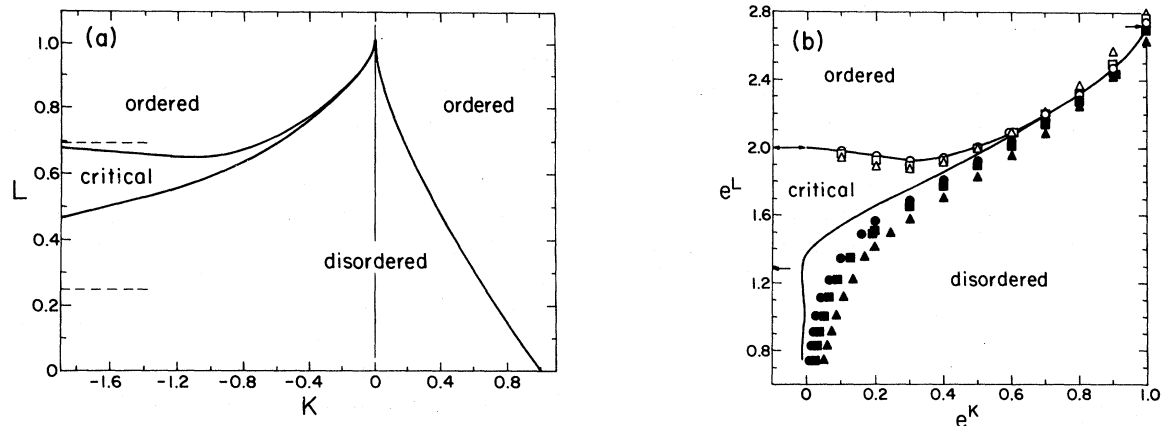


FIG. 1. Phase diagram of three-state Potts model with nearest-neighbor interaction  $K$  and next-nearest-neighbor interaction  $L$  as determined by finite-size scaling. Solid lines are extrapolated values. Dashed lines in (a) are the asymptotes of the critical fan in the limit of infinitely negative  $K$ . Details in this region are shown in (b). Results are shown from pairs of strips of widths  $\frac{4}{2}$  (triangles),  $\frac{6}{4}$  (squares),  $\frac{8}{6}$  (circles). Arrows indicate exact values.

## II. THEORY

The reduced Hamiltonian ( $\mathcal{H} = -H/k_B T$ ) of the three-state Potts model on a square lattice can be written in terms of angle variables  $\theta_i$  at site  $i$ :

$$\mathcal{H} = \sum_{\langle ij \rangle} \frac{2}{3} K [\cos(\theta_i - \theta_j) + \frac{1}{2}] + \sum_{(ij)} \frac{2}{3} L [\cos(\theta_i - \theta_j) + \frac{1}{2}] + h_S \left[ \sum_i \cos\theta_i - \sum_j \cos\theta_j \right] + h_D \left[ \sum_i \cos\theta_i + \sum_j \cos\theta_j \right], \quad (2.1)$$

where  $\theta_i = 0, \pm 2\pi/3$ . The first and second sums are over nearest- and next-nearest-neighbor pairs, respectively, of the square lattice. In the third and fourth terms the square lattice has been decomposed into two sublattices of next-nearest-neighbor sites with index  $i$  ranging over all sites of one sublattice and  $j$  over the other. Thus  $h_S$  is a staggered field that favors different angles, or "colors," on the two sublattices, and  $h_D$  is a direct field favoring the same color on the sublattices. For the case of the antiferromagnetic Potts model for which  $K < 0$ , it is convenient to make the change of variable

$$\theta_i \rightarrow \theta_i, \quad i \text{ on sublattice 1}$$

$$\theta_i \rightarrow \theta_i - \pi, \quad i \text{ on sublattice 2}$$

which leads to

$$\mathcal{H} = \sum_{\langle ij \rangle} \left(-\frac{2}{3}K\right) [\cos(\theta_i - \theta_j) - \frac{1}{2}] + \sum_{(ij)} \frac{2}{3} L [\cos(\theta_i - \theta_j) + \frac{1}{2}] + h_S \left[ \sum_i \cos\theta_i + \sum_j \cos\theta_j \right] + h_D \left[ \sum_i \cos\theta_i - \sum_j \cos\theta_j \right]. \quad (2.2)$$

For the antiferromagnetic Potts model the interaction is now ferromagnetic between nearest-neighbor variables.

We first consider the system in the absence of fields and in the limit  $K \rightarrow -\infty$ . The difference between nearest-neighbor variables, modulo  $2\pi$ , is thereby restricted to the values  $\pm\pi/3$ . A three-to-one mapping to an  $F$  model<sup>3</sup> on the dual lattice is obtained by assigning arrows to the links of the dual lattice according to the following rule: As one looks from the tail to the tip of the arrow, the difference between the angle on the left and the angle on the right, modulo  $2\pi$ , is  $\pi/3$ . The six configurations of the resulting  $F$  model with their Boltzmann weights in terms of  $v \equiv e^L$  are shown in Fig. 2.

The single parameter  $\Delta$  of the  $F$  model<sup>3</sup> is defined in terms of a temperaturelike variable  $R$ , the ratio of the Boltzmann weight of the first four configurations to that of the other two, or  $\Delta = 1 - 1/2R^2$ . With the weights given in Fig. 2 we have

$$\Delta = 1 - v^2/2. \quad (2.3)$$

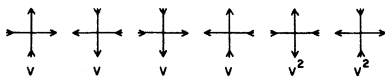


FIG. 2.  $F$ -model vertices and their Boltzmann weights.

From the exact solution<sup>3</sup> we know that the  $F$  model is critical for  $|\Delta| \leq 1$  corresponding to  $0 \leq v \leq v_2$ , where  $v_2 = 2$ . For  $\Delta < -1$  corresponding to  $v > v_2$ , the  $F$  model undergoes an infinite-order (Kosterlitz-Thouless) transition to an antiferroelectric ordered state. The two states of the antiferroelectric correspond in the three-to-one mapping to the six states of the Potts model in which one color occupies one sublattice and another color occupies the other. The particular  $F$  model obtained for the value  $\Delta = \frac{1}{2}$  is called the "square-ice" model and corresponds to the antiferromagnetic Potts model with infinite nearest-neighbor repulsion only. This correspondence has been known for some time.<sup>1</sup>

We now relax the restriction of infinite-strength nearest-neighbor interactions. With  $K$  finite, nearest-neighbor angles can differ by  $\pm\pi$  corresponding to the same Potts color occupying adjacent sites. This configuration can be indicated in the vertex model by an impurity or zero occupying the link of the dual lattice. In this way the Potts model is mapped to a 27-vertex model. The kinds of allowed vertices, the number of each, and their Boltzmann weight are shown in Fig. 3, where  $u = e^K$ .

To determine how the symmetry of the  $F$  model is broken by the temperature field in the limit  $u \ll 1$  it is sufficient to consider only the three

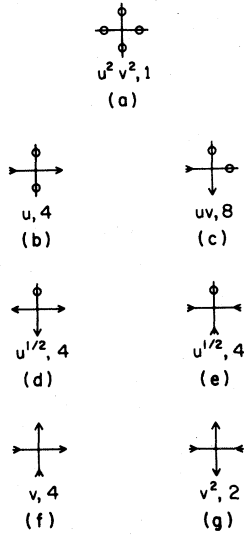


FIG. 3. 27-vertex representation of the three-state Potts model: the vertices, their Boltzmann weights, and the number of each.

kinds of bound pairs of vortex states [Figs. 3(d) and 3(e)], which are shown in Figs. 4(a)–4(c) together with the number of each.

Note that the first two excitations shown have a net flux of arrows and thus violate the ice rule, whereas the third excitation does not. These bound pairs which involve an impurity can be placed in one-to-one correspondence with the more usual excitations of vertex models by the convention of replacing an impurity on a vertical bond by an upward-pointing arrow and an impurity on a horizontal bond by a right-pointing arrow, as shown in Figs. 4(d)–4(g). From this figure it is seen that the excitations are equivalent to bound pairs of vortices with a net flux of four arrows [Figs. 5(a) and 5(b)] or two arrows [Figs. 5(c) and 5(d)].

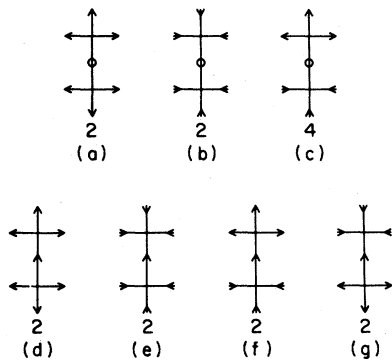


FIG. 4. (a)–(c) The possible bound pairs of vertices in Figs. 3(d) and 3(e). The number of each is shown. (d)–(g) Same bound pairs after replacement of the zero by an arrow. The number of each is shown.

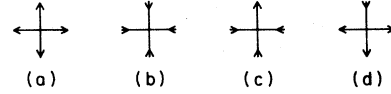


FIG. 5. The excitations of Figs. 4(d)–4(g) are bound pairs of vertices shown.

The former are excitations of the  $F$  model which enlarge it to the eight-vertex model while the latter enlarge it to the more general 16-vertex model. The scaling indices of the operators which create these excitations are known through several studies relating the  $F$  model and its excitations to the Gaussian model and its excitations.<sup>10–17</sup> The scaling indices of the latter can be calculated directly.<sup>10</sup> For our purposes the most convenient of these studies is that of Knops,<sup>17</sup> who considers the renormalization of the body-centered solid-on-solid (BCSOS) model to the Gaussian model. The former is equivalent to the  $F$  model.<sup>20</sup> The vertices of Fig. 5, which represent screw dislocations in the BCSOS model, and the operators of the Gaussian model to which they correspond, are considered explicitly by Knops. The results are straightforward. Consider first the vertices of Figs. 5(a) and 5(b). From our rule that the angles of Eq. (2.2) increase by  $\pi/3$  when crossing an outward-pointing arrow from right to left it can be seen that these configurations correspond to vortices of strength  $\pm \frac{2}{3}$  in units of  $2\pi$ . Similarly the configurations of Figs. 5(c) and 5(d) correspond to vortices of strength  $\pm \frac{1}{3}$ . In the notation of Kadanoff<sup>10</sup> they correspond to the Gaussian operators  $S_{0,2/3}$  and  $S_{0,1/3}$  with scaling indices  $x_{0,2/3}$  and  $x_{0,1/3}$ . As noted above, the excitations of the  $F$  model which lead to the antiferromagnetic Potts model can be considered to be bound pairs of these configurations. Thus the excitations of Figs. 4(d) and 4(e) have vorticity of  $\pm 1$  corresponding to  $S_{0,1}$  with scaling index  $x_{0,1}$ . The scaling indices  $x_{n,m}$  can be calculated explicitly in terms of the strength of the coupling of the Gaussian model  $K_G$  as<sup>10</sup>

$$x_{n,m} = \frac{n^2}{4\pi K_G} + m^2 \pi K_G. \quad (2.4)$$

*A priori*, one does not know the value of the coupling of the Gaussian model to which one renormalizes so that absolute values of these indices cannot be obtained. Nevertheless, very useful relations follow between indices, such as

$$x_{0,1} = \frac{9}{4} x_{0,2/3}. \quad (2.5)$$

Fortunately, for the case of the  $F$  model the scaling index of the operator  $S_{0,2/3}$  which enlarges its space

to that of the eight-vertex model are known from Baxter's solution of that model.<sup>18</sup> Thus

$$x_{0,2/3} = 2 - y_{8V}, \quad (2.6)$$

where

$$y_{8V} = \frac{2}{\pi} \cos^{-1}(-\Delta), \quad (2.7)$$

with  $0 < y_{8V} < 2$ . We combine Eqs. (2.5)–(2.7) to obtain the critical index  $y_K \equiv 2 - x_{0,1}$  as

$$(2 - y_K) = \frac{9}{4}(2 - y_{8V})$$

or

$$y_K = \frac{9}{2\pi} \cos^{-1} \left[ \frac{v^2}{2} - 1 \right] - \frac{5}{2}, \quad (2.8)$$

in which  $-\frac{5}{2} < y_K < 2$ , where Eq. (2.3) has been used.

In the limit  $u \rightarrow 0$  the free energy  $f(u, v)$  will behave as

$$f(u, v) \sim u^{2/y_K(u)}$$

in the range of  $u$  where these excitations are relevant. From Eq. (2.8) this is seen to be for all

$$v < v_1 = (2 + 2 \cos 5\pi/9)^{1/2},$$

which is approximately 1.29. Thus the line  $u = 0$  is unstable with respect to these excitations for all  $v < v_1$  and the Potts model is disordered for any nonzero value of temperature. In particular this is true for the model with nearest-neighbor interactions only ( $v = 1$ ). We see that this model has a transition only at zero temperature and that its free energy behaves like  $f(K) \sim e^{4K}$ .

For small  $u$  the antiferromagnetic Potts model undergoes a Kosterlitz-Thouless transition to a critical phase at  $v \simeq v_1$ , where the excitations become marginal. The critical phase persists until  $v \simeq v_2 = 2$ . Thus the presence of the critical phase in the antiferromagnetic Potts model is established. In the critical phase the excitations of Figs. 4(a) and 4(b) occur only in bound pairs, with total vorticity zero. For completeness we remark that excitations in Fig. 4(c), having no vorticity, do not affect the renormalization flow of the  $F$  model to the Gaussian model except for a trivial renormalization of the Gaussian coupling constant. We also note that the excitations of Figs. 3(a)–3(c), heretofore neglected, do not affect the leading singular behavior of the free energy. This can be seen from the fact that the excitations obey the ice rule (zero flux of arrows) so that any aggregate of them has no topological consequence. Only the vertices of Figs. 3(d) and

3(e) are impurity sources, or sinks, and must be present in pairs in any island of excitations. Such an island must have a net flux of arrows of zero or a multiple of six corresponding to integer vorticity. However, the scaling indices  $x_{n,m}$  increase with increasing vorticity, indicating that the most relevant excitation is that with unit vorticity, which we have treated. Further, excitations with smaller vorticity cannot be created by pulling apart the bound pairs of Figs. 4(a)–4(c), for in doing so one generates (at least) a string of zeros. Thus the pair is confined with a linear potential.

The power-law decay of the Potts color-color correlation function in the critical region can be obtained by considerations similar to those leading to  $y_K$ . The correlation function can be written

$$\langle \cos(\theta_i - \theta_j) \rangle \sim \frac{A}{r^{2x_D}} \pm \frac{B}{r^{2x_S}},$$

where  $r$  is the distance between sites  $i$  and  $j$  and the sign of the second term depends on whether  $i, j$  are on the same or different sublattices. The scaling index  $x_S$  of the staggered field is obtained by noting from Eq. (2.2) that the staggered field  $h_S$  couples to

$$S_{1,0} = \sum_i \cos \theta_i + \sum_j \cos \theta_j,$$

which identifies  $x_S = x_{1,0}$ . The direct field  $h_D$  couples to the staggered operator

$$S_{1,0}^S = \sum_i \cos \theta_i - \sum_j \cos \theta_j.$$

Under renormalization this generates the operator  $S_{2,0}$  from which  $x_D = x_{2,0}$ . From the general expression for  $x_{n,m}$  in (2.4) we obtain the following results:

$$\begin{aligned} x_D &= x_{2,0} \\ &= 4x_{1,0}, \end{aligned}$$

or

$$x_D = 4x_S \quad (2.9)$$

and

$$x_{1,0} x_{0,1} = \frac{1}{4},$$

from which

$$x_S(2 - y_K) = \frac{1}{4}, \quad (2.10)$$

with  $y_K$  given by (2.8). In the critical fan,  $-\frac{5}{2} \leq y_K \leq 0$ , so that  $\frac{1}{18} \leq x_S \leq \frac{1}{8}$  and  $\frac{2}{9} \leq x_D \leq \frac{1}{2}$ . In particular, at the ice point,  $y_K = \frac{1}{2}$ , so that  $x_D = \frac{2}{3}$ , in agreement with the exact results of Baxter<sup>21</sup> at this point.

Note that not only the staggered field but also the direct field is relevant. The favoring of one color by such a field causes a crossover from the universality class of the six-state clock model to that of two nondegenerate Ising models with four-spin coupling.<sup>22</sup> Of the six original ground states, the four containing the favored color are reached by a sequence of two Ising transitions. If the direct field disfavors one color, then, of the original six states, the two which do not contain this color dominate and a single Ising transition to them takes place.

The phase boundaries of the system are now known along the line  $e^K=0$ . Two other points on the phase boundaries in the  $(K,L)$  plane are known exactly. They are the transition temperature of the ferromagnetic Potts model with nearest-neighbor interactions only, which is  $(C,0)$  with  $C=\ln(1+\sqrt{3})$ , and that of the decoupled ferromagnetic sublattices  $(0,C)$ . The thermal and magnetic critical indices along the ferromagnetic phase boundary up to and including the decoupling point  $(0,C)$  take the values<sup>23</sup>  $y_T=\frac{6}{5}$ ,  $y_H=\frac{28}{15}$ . At the decoupling point the field  $K$  is relevant with crossover exponent<sup>24</sup>

$$\phi \equiv (2y_H - 2)/y_T = \frac{13}{9}.$$

It follows that, in the neighborhood of this point, the phase boundary shows a cusp of the form<sup>24</sup>  $K \sim (L - C)^\phi$ . For  $L > C$  and  $K = 0$  there is a first-order transition between the ferromagnetic and anti-ferromagnetic regions. An interesting question is whether the critical phase exists all the way to the decoupling point, making it a form of bicritical

point, or terminates elsewhere. In this latter case we expect a single line of first-order transitions joining this point of termination to the decoupling point, making it a critical end point. To explore this question, to determine the phase boundaries themselves, and to verify the prediction of Eq. (2.8) we turn to an approximate calculation employing the phenomenological renormalization-group technique.<sup>19</sup>

### III. FINITE-SIZE CALCULATION

#### A. Method

In this section we present the result of a finite-size calculation. The phase diagram of the three-state Potts model with arbitrary nearest-neighbor interaction  $K$  and ferromagnetic interaction  $L$  is obtained. As we have shown above, the existence of a critical fan is a consequence of the precise dependence on  $L$  of the exponent  $y_K$  at  $e^K=0$ . We shall numerically check the predicted relation between  $y_K$  and the temperature exponent  $y_{8V}$  of the eight-vertex model. For our calculations we employ an adapted version of the phenomenological renormalization method.<sup>19</sup>

Consider a Potts system on a strip of  $m$  columns each of height  $n$  in the limit  $m \rightarrow \infty$ . Most of our calculations are based on finite-size scaling properties of the interface free energy. This quantity may be obtained as the difference in free energy of system with periodic boundary conditions with and without a step. To be precise, we consider the following Hamiltonian [cf. Eq. (2.1)]:

$$\mathcal{H} = \frac{2}{3} \sum_{i=1}^n \sum_{j=1}^m \{ K [\cos(\theta_{i,j} - \theta_{i,j+1}) + \cos(\theta_{i,j} - \theta_{i+1,j} - \Delta_i) + 1] \\ + L [\cos(\theta_{i,j} - \theta_{i+1,j-1} - \Delta_i) + \cos(\theta_{i,j} - \theta_{i+1,j+1} - \Delta_i) + 1] \}, \quad (3.1)$$

where each site is now labeled by two indices and  $i+n \equiv i$ ,  $j+m \equiv j$ , and  $\Delta_i = 0$  for  $i=1, \dots, n-1$  and  $\Delta_n = (2\pi/3)\Delta$ . The cases  $\Delta=1$  and  $\Delta=0$  yield periodic boundary conditions with and without a step, respectively.

A transfer matrix  $T^\Delta$  can be introduced (see the Appendix) with eigenvalues  $\lambda_0^\Delta > |\lambda_1^\Delta| \geq \dots$ . The dimensionless free energy per column is given by

$$f_n^\Delta = -\ln \lambda_0^\Delta, \quad (3.2)$$

and the interface free energy per spin by

$$\hat{\kappa}_n = f_n^1 - f_n^0 = \ln \lambda_0^0 / \lambda_0^1. \quad (3.3)$$

In two dimensions the interface free energy satisfies the scaling equation

$$\hat{\kappa}_n = b^{-1} \hat{\kappa}'_{n/b}, \quad (3.4)$$

where  $b$  is an arbitrary scaling length, and the prime at the right-hand side indicates that the quantity is evaluated with scaled interaction parameters. This relation implies that at a critical point

$$\hat{\kappa}_n \sim n^{-1}. \quad (3.5)$$

On general grounds the interface free energy is expected to behave like

$$\hat{\kappa}_n = \hat{\kappa}_\infty + O(e^{-n/\xi}) \quad (3.6)$$

in the ordered regime and

$$\hat{\kappa}_n = O(e^{-n/\xi}) \quad (3.7)$$

in the disordered regime; we have denoted by  $\xi$  the correlation length of the system in the thermodynamic limit.

To locate critical points we compare two systems, of size  $n$  and  $n-p$ . Since two-sublattice fluctuations dominate in the present model, we take  $p=2$ . The various types of behavior of  $\hat{\kappa}_n$  may conveniently be described by an effective exponent

$$y_{\text{eff}} = -\frac{\ln \hat{\kappa}_n / \hat{\kappa}_{n-p}}{\ln(n/n-p)}. \quad (3.8)$$

One finds

$$y_{\text{eff}} \sim n, \quad (3.9)$$

$$y_{\text{eff}} \simeq 1, \quad (3.10)$$

$$y_{\text{eff}} \sim e^{-n/\xi}, \quad (3.11)$$

in the disordered, critical, and ordered regions, respectively.

Finally, we write  $y_\epsilon$  for the critical exponent describing the dominant critical behavior associated with a deviation from criticality due to a change in some parameter  $\epsilon$ . The exponent  $y_\epsilon$  may then be obtained, as usual, from  $\hat{\kappa}_n^{(l)}$ , the derivative of order  $l$  of  $\hat{\kappa}_n$  with respect to  $\epsilon$ , using the relation

$$\hat{\kappa}_n^{(l)} \sim n^{y_\epsilon - 1}, \quad (3.12)$$

i.e.,

$$y_\epsilon = \frac{1}{l} \left[ \frac{\ln \hat{\kappa}_n^{(l)} / \hat{\kappa}_{n-p}^{(l)}}{\ln(n/n-p)} + 1 \right]. \quad (3.13)$$

Provided the following changes are made, all relations above also hold with  $\hat{\kappa}_n$  replaced by  $\kappa_n$ , the inverse correlation length defined in terms of the two dominant eigenvalues of the transfer matrix

$$\kappa_n = \ln |\lambda_0^0 / \lambda_1^0|. \quad (3.14)$$

In Eqs. (3.6) and (3.7), and similarly for (3.9) and (3.11), "order" and "disorder" have to be interchanged, i.e.,

$$\kappa_n = \kappa_\infty + O(e^{-n/\xi}) \quad (3.15)$$

in the disordered region, and

$$\kappa_n = O(e^{-n/\xi}) \quad (3.16)$$

in the ordered region. Furthermore, Eq. (3.16) holds only if  $\lambda_0^0$  and  $\lambda_1^0$  are degenerate in the thermodynamic limit. This occurs if  $\kappa_n$  describes the decay of order-parameter—order-parameter correlations. Otherwise Eq. (3.15) also applies in this case. Our numerical calculations indicate that either of these possibilities may be realized in the Potts model, depending on the nature of the ordered state. In particular, Eq. (3.16) applies in the antiferroelectrically ordered portion of the phase diagram. However, close to the  $F$ -model transition at  $e^K=0$ ,  $\kappa_n$  shows a minimum as a function of  $e^K$  indicating that  $\kappa_n$  approaches a finite, nonzero value as  $n \rightarrow \infty$  in the unphysical region  $e^K < 0$ .

## B. Results

The phase diagram shown in Fig. 1 was obtained as follows. For ferromagnetic nearest-neighbor interactions ( $e^K > 1$ ) the critical curve is the solution to Eq. (3.8) with  $y_{\text{eff}}=1$ , which thereby reduces to the usual phenomenological renormalization criterion applied to the interface free energy.

To obtain the boundaries of the critical phase for antiferromagnetic nearest-neighbor interactions ( $e^K < 1$ ) the following observation was made. Suppose Eq. (3.8) is solved with the effective exponent  $y_{\text{eff}}$  set equal to  $1+\delta$ . It then follows from Eqs. (3.9)–(3.11) that for  $n \rightarrow \infty$  and  $\delta > 0$ , one will obtain the boundary between the disordered and critical phases. Similarly, for  $-1 < \delta < 0$  one will obtain the boundary between the ordered and critical phases. The calculations showed fastest convergence with  $\delta$  chosen as follows: (i)  $\delta=0$  for the left-hand boundary, and (ii)  $\delta=\delta_n$  such that the known critical point  $e^K=0$ ,  $L=\ln 2$  of the  $F$  model on the boundary between critical and ordered phases is exactly reproduced. In passing we note that  $\delta_n$  defined thus depends surprisingly regularly on  $n$ :  $\delta_n = 1 - a/n$  with  $a = 0.688, 0.642, \text{ and } 0.638$  for  $n = 4, 6, \text{ and } 8$ .

Figure 1 shows the critical surface, based on data points for  $n = 4, 6, \text{ and } 8$ . The solid curve is the result of a three-point power-law extrapolation (where possible); i.e., three successive points of a given sequence  $a_n$  are fitted to the form

$$a_n = a_\infty + \alpha n^{-\beta}. \quad (3.17)$$

Where no such extrapolation was possible the  $n = 8$  estimate was used instead. For ordinary critical points this type of extrapolation is very accurate.<sup>25</sup> Owing to the presence of a marginal exponent in the critical phase, the dominant singularity due to

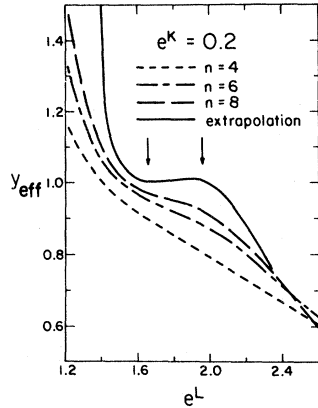


FIG. 6. Effective exponent defined in Eq. (3.8) vs  $e^L$  for a fixed  $K$ . Critical points are identified by  $y_{\text{eff}} \approx 1$ . Arrows indicate boundaries of critical regions as given in Fig. 1.

corrections to scaling for large  $n$  is logarithmic rather than of the form of (3.17). Still, for small  $n$  this expression is expected to be appropriate.

The results in Fig. 1 seem to indicate that the critical phase disappears for  $e^K \gtrsim 0.6$ . We have not been able to determine the nature of the transition for  $0.6 \lesssim e^K < 1$ . As noted earlier, we expect that either the critical fan continues or there is a single first-order transition. Close to the decoupling point the critical surface has a cusp<sup>24</sup> and can be represented to within 1% by

$$K = \begin{cases} [C - L(K)]^\phi & \text{for } K > 0 \\ -\{2[C - L(K)]\}^\phi & \text{for } K < 0 \end{cases}$$

where  $C = \ln(\sqrt{3} + 1)$  and

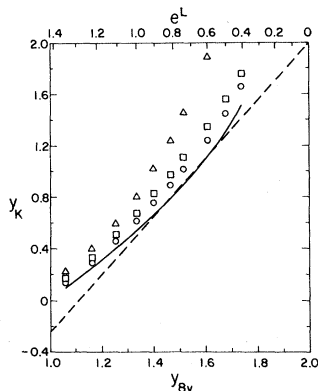


FIG. 7. Critical index  $y_K$  at  $e^K=0$ . It is shown as a function of  $y_{8\nu}(L)$  and of  $e^L$ . Results are shown from pairs of widths  $\frac{4}{2}$  (triangles),  $\frac{6}{4}$  (squares),  $\frac{8}{6}$  (circles). The solid line is obtained by extrapolation. The dashed straight line is the predicted extended scaling relation Eq. (1.1).

TABLE I. Values of the magnetic exponents  $y_S, y_D$  at the boundaries of the critical fan. Exact values are from Eqs. (2.9) and (2.10) (and  $y = 2 - x$ ).

$e^K$	$e^L$	4-2	6-4	8-6	Exact
Staggered magnetic exponent					
0.2	1.66	1.867	1.876	1.884	1.875
	1.95	1.932	1.934	1.937	1.944
0.3	1.75	1.882	1.882	1.887	1.875
	1.92	1.935	1.931	1.931	1.944
Direct magnetic exponent					
0.2	1.66	1.617	1.597	1.591	1.5
	1.95	1.727	1.718	1.717	1.778
0.3	1.75	1.636	1.604	1.595	1.5
	1.92	1.704	1.684	1.680	1.778

$$\phi = (2y_H - 2)/y_T = \frac{13}{9}.$$

In the neighborhood of the pure Potts model to within 0.1% one has

$$K(L) = C - \frac{1}{2}(\sqrt{3} + 1)L.$$

Figure 6 displays the behavior of the effective exponent  $y_{\text{eff}}$ , Eq. (3.8), which is crucial in determining the phase diagram. We plot  $y_{\text{eff}}$  as a function of  $L$  for  $e^K=0.2$ , again for  $n=4, 6$ , and  $8$  and extrapolated as above. The flat portion in the extrapolated curve at  $y_{\text{eff}}=1$  is a clear signature of a critical phase, and the phase boundaries as obtained above are indicated by arrows.

Figure 7 is a plot of  $y_K$  as a function of  $y_{8\nu}$ . The estimates of  $y_K$  were obtained by applying Eq. (3.13) to the second-order derivative of  $\hat{\kappa}_n$  with respect to  $e^K$ . Again there are results for  $n=4, 6$ , and  $8$  and the power-law extrapolation. The first-order derivative also might have been used to calculate  $y_K$ . However, its behavior is irregular, possibly indicating a vanishing amplitude in Eq. (3.12). The numerical results for  $y_K$  match well with the theoretically predicted straight line. The deviations for small, positive  $y_K$  reflect the failure of our method to produce irrelevant exponents.

The staggered and direct magnetic exponents  $y_S = 2 - x_S$  and  $y_D = 2 - x_D$  were also calculated, at the phase boundaries of the critical fan. The direct and staggered exponents were obtained from the first and second derivatives of  $\kappa$ , respectively. The results for various values of  $e^K$  are contained in Table I. Again the numerical results compare favorably with our theoretical prediction.

#### IV. PHYSICAL REALIZATION

Direct physical realizations of the two-dimensional antiferromagnetic three-state Potts model are limited to the adsorption of ternary alloys or square substrates. However, realizations of the universality class of the six-state clock model are much less restricted. For example, the triangular Ising antiferromagnetic can exhibit, in zero field, a transition in this universality class<sup>26</sup> and is more readily realized physically due to the triangular symmetry. As is well known, the antiferromagnetic triangular Ising model in the form of the lattice gas to which it is equivalent can be used to describe the order-disorder transition to the  $\sqrt{3} \times \sqrt{3}$  phase exhibited by some noble gases on graphite.<sup>27</sup> However, the condition of zero magnetic field implies equal numbers of occupied and unoccupied sites or a density  $n = \frac{1}{2}$  which is far in excess of the densities  $n \lesssim \frac{1}{3}$  for which the lattice-gas description is adequate for these systems. A second possibility, not subject to this difficulty, is a two-component mixture on a triangular lattice. To be specific, we consider a mixture of krypton and xenon adsorbed on graphite in a  $\sqrt{3} \times \sqrt{3}$  phase.<sup>28</sup> As both krypton<sup>29</sup> and xenon<sup>30</sup> have been observed to order in such a phase it is likely that a mixture will also order. The transition to this state is not of interest here but rather the compositional ordering which will take place at lower temperatures. The mixture on the triangular lattice (with lattice constant 4.26 Å) is readily mapped onto an Ising model with coupling

$$J(r) = -[V_{KK}(r) + V_{XX}(r) - 2V_{KX}(r)]/4,$$

where  $V_{KK}$  is the strength of the krypton-krypton interaction at 4.26 Å and similarly for the other interactions. If  $J(4.26)$  is positive the Ising model is ferromagnetic and the mixture undergoes a simple phase separation at low temperatures. However, if  $J(4.26)$  is negative the Ising model is antiferromagnetic and at low temperatures the system will order into a phase in which the more numerous component occupies two sublattices and the less numerous component a single sublattice. We thus have an antiferromagnetic triangular Ising model with the advantage that the condition of zero field here merely implies an equal number of krypton and xenon atoms, a situation easily prepared.

If we use the standard Lennard-Jones 6-12 potentials for the needed interactions<sup>31</sup> and the usual combining rules for the strength<sup>32</sup>  $\epsilon_{KX}$

$=(\epsilon_{XX}\epsilon_{KK})^{1/2}$  and range  $\sigma_{KX} = \frac{1}{2}(\sigma_{XX} + \sigma_{KK})$  we find  $J(4.26)/k_B = -16$  K as desired. The negative sign indicates that the xenon and krypton atoms prefer to sit next to one another rather than next to one of their own species. This preference arises from the fact that the natural spacing of the xenon is somewhat larger than the 4.26 Å provided by the graphite, whereas that of the krypton is somewhat smaller. The preferred separation of a krypton-xenon pair, then, is quite close to the graphite spacing.

A schematic phase diagram<sup>33</sup> of the system is shown in Fig. 8. Note again that *disordered* refers to the compositionally disordered ( $\sqrt{3} \times \sqrt{3}$ ) triangular lattice. The maximum transition temperature to the ordered states, which occur at compositions of  $\frac{1}{3}$  and  $\frac{2}{3}$ , is set by  $J(4.26)$  and can be estimated<sup>27</sup> as  $1.4 |J(4.26)|/k_B \approx 22$  K. These transitions are in the universality class of the three-state Potts model. The scale of the transitions to the critical phase at composition  $\frac{1}{2}$  is set by  $J(r)$  evaluated at the second-neighbor distance of 7.38 Å, which is  $J(7.38)/k_B = 0.7$  K. The sign indicates the second-neighbor interaction is ferromagnetic, which, as in the Potts antiferromagnet, makes the transition temperature to the critical phase nonzero. We expect it to be of the order of 1 K. The signature of the critical phase would be seen in the behavior of the exponent  $\beta$  which governs the disappearance of the scattering intensity from the superlattice spots upon crossing a continuous-phase-transition boundary. Whereas  $\beta = \frac{1}{9}$  whenever the boundary separating the ordered and disordered phases is crossed, we expect  $\beta$  to vary continuously with temperature whenever the critical phase boundary at concentration of  $\frac{1}{2}$  is traversed.

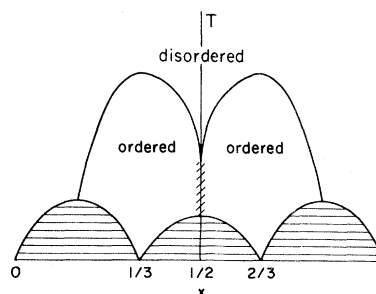


FIG. 8. Schematic phase diagram in the temperature-composition plane of a krypton-xenon mixture adsorbed on graphite in a triangular  $\sqrt{3} \times \sqrt{3}$  array. The compositionally ordered phases are shown; horizontal lines denote regions of two-phase coexistence, and the critical phase is indicated by the cross-hatching at  $x = \frac{1}{2}$ .

ACKNOWLEDGMENTS

We wish to acknowledge useful conversations with J. R. Banavar, J. G. Dash, E. Domany, S. C. Fain, G. S. Grest, L. P. Kadanoff, and S. H. Shenker. This work was supported in part by the National Science Foundation under Grant No. DMR-79-20785.

APPENDIX

In this appendix, various techniques to make the transfer matrix numerically tractable are described. A factorization into sparse matrices was carried out. Denote by  $\langle s_i, s_{i+1} | E | t_i, t_{i+1} \rangle$  the contribution to the total Hamiltonian associated with the four spins  $s_i, s_{i+1}, t_i$ , and  $t_{i+1}$  in an elementary square. The transfer matrix element connecting the columns  $s_1, \dots, s_n$  and  $t_1, \dots, t_n$  then can be written in the form

$$\langle s_1, \dots, s_n | T | t_1, \dots, t_n \rangle = \prod_{i=1}^n \exp \langle s_i, s_{i+1} | E | t_i, t_{i+1} \rangle .$$

Using the symbolic notation

$$\exp \langle s_i, s_{i+1} | E | t_i, t_{i+1} \rangle = \begin{array}{ccc} \circ & & \circ \\ | & \diagdown & / \\ \bullet & & \bullet \\ | & / & \diagdown \\ \bullet & & \bullet \end{array} ,$$

one has

$$\langle s_1, \dots, s_n | T | t_1, \dots, t_n \rangle = \begin{array}{ccccccc} \circ & & \circ & & \circ & \dots & \circ \\ | & \diagdown & / & & | & & | \\ \bullet & & \bullet & & \bullet & \dots & \bullet \\ | & / & \diagdown & & | & & | \\ \bullet & & \bullet & & \bullet & & \bullet \end{array} .$$

The transfer matrix can be factorized into

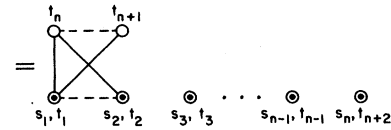
$$T = PQ^{n-3}Q'R, \tag{A1}$$

where the matrices on the right-hand side are defined as follows:

$$\begin{aligned} \text{(i)} \quad & \langle s_1, \dots, s_n | P | t_1, \dots, t_n, t_{n+1}, t_{n+2} \rangle \\ & = \delta_{s_1, t_1} \delta_{s_2, t_2} \dots \delta_{s_{n-1}, t_{n-1}} \delta_{s_n, t_{n+2}} \\ & \quad \times \exp \langle s_1, s_2 | E | t_n, t_{n+1} \rangle . \end{aligned}$$

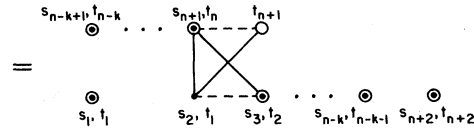
Representing, as above, the  $s_i$  by large dots and the  $t_i$  by circles, one obtains a graph:

$$\langle s_1, \dots, s_n | P | t_1, \dots, t_{n+2} \rangle$$

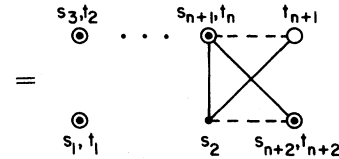


Note that coinciding dots and circles represent a Kronecker  $\delta$  function.

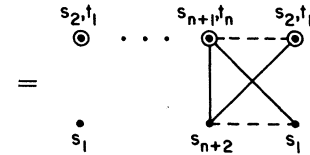
$$\text{(ii)} \quad \langle s_1, \dots, s_{n+2} | Q | t_1, \dots, t_{n+2} \rangle$$



$$\text{(iii)} \quad \langle s_1, \dots, s_{n+2} | Q' | t_1, \dots, t_{n+2} \rangle$$



$$\text{(iv)} \quad \langle s_1, \dots, s_{n+2} | R | t_1, \dots, t_n \rangle$$



Note that in the product (A1) there are  $q^{n+2}$  intermediate states of  $n+2$  spins for a general  $q$ -state Potts model. However, the matrix factors decompose into  $q^2$  blocks corresponding to different values of  $s_1$  and  $s_n$ , reducing the number of intermediate results to be stored simultaneously in the computer to  $q^n$ .

For the computation of the largest eigenvalue of the transfer matrix we used the conjugate gradient method. The corresponding eigenvector, which is obtained at the same time, allowed us to calculate first-order derivatives with perturbation theory. The numerical solution of the equation  $y_{\text{eff}} = \text{const}$  (for the calculation of the critical surface) could thereby be performed very efficiently with Newton's method. The number of components of the eigenvector may be reduced (by a factor  $q$ ) using color-permutation symmetry by only calculating one vector element of all those which are equal by symmetry. Note that the intermediate states in (A1) lack this symmetry.

- <sup>1</sup>The correspondence of the three-coloring problem to the square-ice model is usually attributed to Lennard; see, e.g., E. H. Lieb, *Phys. Rev. Lett.* **18**, 692 (1967).
- <sup>2</sup>A. N. Berker and L. P. Kadanoff, *J. Phys. A* **13**, L259 (1980).
- <sup>3</sup>E. H. Lieb, *Phys. Rev. Lett.* **18**, 1046 (1967).
- <sup>4</sup>R. J. Baxter (unpublished).
- <sup>5</sup>J. Cardy, *Phys. Rev. B* **24**, 5128 (1981).
- <sup>6</sup>J. M. Kosterlitz and D. J. Thouless, *J. Phys. C* **6**, 1181 (1973). For a discussion of the clock model, see J. José, L. P. Kadanoff, S. Kirkpatrick, and D. R. Nelson, *Phys. Rev. B* **16**, 1217 (1977); S. Elitzur, R. B. Pearson, and J. Shigemitsu, *Phys. Rev. D* **19**, 3698 (1979).
- <sup>7</sup>G. S. Grest and J. R. Banavar, *Phys. Rev. Lett.* **46**, 1458 (1981).
- <sup>8</sup>M. P. Nightingale and M. Schick, *J. Phys. A* **15**, L39 (1982).
- <sup>9</sup>C. Jayaprakash and J. Tobochnik *Phys. Rev. B* **25**, 4890 (1982).
- <sup>10</sup>L. P. Kadanoff and A. C. Brown, *Ann. Phys. (N.Y.)* **121**, 318 (1979).
- <sup>11</sup>A. M. M. Pruisken and L. P. Kadanoff, *Phys. Rev. B* **22**, 5154 (1980).
- <sup>12</sup>A. M. M. Pruisken and A. C. Brown, *Phys. Rev. B* **23**, 1459 (1981).
- <sup>13</sup>A. Luther and I. Peschel, *Phys. Rev. B* **12**, 3908 (1975).
- <sup>14</sup>F. D. M. Haldane, *Phys. Rev. Lett.* **45**, 1358 (1980).
- <sup>15</sup>J. Black and V. J. Emery, *Phys. Rev. B* **23**, 429 (1981).
- <sup>16</sup>M. P. M. den Nijs, *Phys. Rev. B* **23**, 6111 (1981).
- <sup>17</sup>H. Knops, *Ann. Phys. (N.Y.)* **128**, 448 (1981).
- <sup>18</sup>R. J. Baxter, *Ann. Phys. (N.Y.)* **70**, 193 (1972).
- <sup>19</sup>M. P. Nightingale, *Physica A* **82**, 561 (1976); *Proc. K. Ned. Akad. Wet.* **32B**, 235 (1978).
- <sup>20</sup>H. van Beijeren, *Phys. Rev. Lett.* **38**, 993 (1977).
- <sup>21</sup>R. J. Baxter, *J. Math. Phys.* **11**, 3116 (1970).
- <sup>22</sup>F. Y. Wu and K. Y. Lin, *J. Phys. C* **7**, L181 (1974).
- <sup>23</sup>The values quoted are those of the hard-hexagon model which has been solved exactly by R. J. Baxter, *J. Phys. A* **13**, L61 (1980). The transition of this model and that of the three-state ferromagnetic Potts model are in the same universality class. See also M. P. M. den Nijs, *J. Phys. A* **12**, 1857 (1979); B. Nienhuis, E. K. Riedel, and M. Schick, *ibid.* **13**, L189 (1980), R. B. Pearson, *Phys. Rev. B* **22**, 2579 (1980).
- <sup>24</sup>J. M. J. van Leeuwen, *Phys. Rev. Lett.* **34**, 1056 (1975).
- <sup>25</sup>M. P. Nightingale and H. W. J. Blöte, *J. Phys. A* **15**, L33 (1982).
- <sup>26</sup>E. Domany, M. Schick, J. S. Walker, and R. G. Griffiths, *Phys. Rev.* **18**, 2209 (1978); also, S. Alexander and P. Pincus, *J. Phys. A* **13**, 263 (1980).
- <sup>27</sup>M. Schick, J. S. Walker, and M. Wortis, *Phys. Rev. B* **16**, 2205 (1977).
- <sup>28</sup>We are indebted to S. Alexander for bringing this system to our attention.
- <sup>29</sup>See P. M. Horn, R. J. Birgeneau, P. Heiney, and E. M. Hammonds, *Phys. Rev. Lett.* **41**, 961 (1978), and references therein.
- <sup>30</sup>J. A. Venables and P. S. Schabes-Retchkiman, *J. Phys. (Paris) Colloq.* **38**, C4-105 (1977).
- <sup>31</sup>J. O. Hirschfelder, C. F. Curtiss, and R. B. Bird, *Molecular Theory of Gases and Liquids* (Wiley, New York, 1954), p. 1110.
- <sup>32</sup>W. A. Steele, *The Interaction of Gases with Solid Surfaces* (Pergamon, New York, 1974), Chap. 2.
- <sup>33</sup>B. Mihura and D. P. Landau [*Phys. Rev. Lett.* **38**, 977 (1977)] employ Monte Carlo methods to investigate the triangular Ising model with first-neighbor antiferromagnetic and second-neighbor ferromagnetic interactions of equal strength. Their Fig. 3 is analogous to our Fig. 8. Although they do not report detection of transitions to a critical phase at  $x = \frac{1}{2}$ , they observe at the maximum transition temperature on this axis a negative value of  $\alpha$  and a large value of  $\beta$ , which indicate that the transition in the infinite system is of the Kosterlitz-Thouless type.